

SIMULATION OF MICROMETEORITE IMPACTS THROUGH IN SITU DYNAMIC HEATING OF LUNAR SOIL. M. S. Thompson¹, T. J. Zega¹, and J. Y. Howe^{2,3}, ¹Lunar and Planetary Laboratory, Department of Planetary Sciences, University of Arizona, 1629 E. University Blvd, Tucson, AZ 85721. E-mail: mst@lpl.arizona.edu, ²Hitachi High-Technologies Canada Inc. 89 Galaxy Blvd. Suite 14, Rexdale, ON, Canada M9W 6A4, ³Department of Materials Science and Engineering, University of Toronto, 27 King's College Circle, Toronto, ON, Canada M5S 1A1.

Introduction: Soil grains on the surfaces of airless bodies are continually modified by micrometeorite impacts and energetic particles from the solar wind, a process that is collectively known as space weathering [1]. Such interactions result in changes to the microstructural and chemical characteristics of the grains and thus, their optical properties. Grain properties were studied in lunar soils returned by the Apollo missions and in samples recently returned from near-Earth asteroid Itokawa by the Hayabusa mission, e.g., [2-5].

To understand the formation of space weathering features in returned samples, experiments simulating solar wind irradiation and micrometeorite impacts have been performed on a variety of target materials, e.g., [6-8]. These experiments have provided insight into the development of space weathering characteristics in grains on airless body surfaces. However, such investigations are static. Data (images, structural, and chemical information) were collected before and after the simulated weathering process, not throughout. Here we present a new methodology for simulating micrometeorite impact events, through dynamic heating experiments inside the transmission electron microscope (TEM). These in situ experiments enable the direct observation of chemical and structural changes resulting from simulated micrometeorite impacts in real-time.

Samples and Methods: Grains of mature lunar soil 79221 were suspended in methanol and the fine-size fraction was extracted and drop cast onto carbon-coated grids and SiN thermal e-chips for analysis in the TEM. We employed two different methodologies for simulating micrometeorite impacts.

In the first method, we heated the samples incrementally on carbon-coated grids using a Gatan slow-heating stage inside the FEI Titan environmental TEM (ETEM) at Arizona State University. We heated the grains from room temperature to ~1000 °C over the course of 15 minutes. We collected bright-field TEM (BF) images of the material at roughly 150 °C increments over the course of the experiment. We also performed energy-dispersive x-ray spectroscopy (EDS) mapping of the samples before and after heating.

In the second method, we thermally-shocked samples on specialized Hitachi SiN chips to ~1000 °C in <1 second inside the Hitachi HF3300 TEM at the University of Toronto. The HF3300 is equipped with

bright-field (BF), dark-field (DF), and secondary electron (SE) detectors, a silicon-drift EDS detector, and a Gatan GIF Quantum electron energy-loss spectrometer (EELS). We recorded video of the heating experiments, and collected BF, high-angle annular dark-field (HAADF), and SE images, as well as EDS maps of the grains before and after heating. We also acquired EELS spectra of several Fe nanoparticles that formed during heating. Spectra were acquired with a dispersion of 0.25 eV/channel and dwell times between 1.0 to 2.0 s/px to determine the oxidation state of Fe in the nanoparticles. We subjected some of the samples to multiple heating events, repeatedly thermally shocking them to ~1000 °C in <1 s as many as eight times. We recorded video throughout each heating interval, and imaged and collected EDS maps of the grains after the final thermal event.

Results and Discussion: We monitored individual grains throughout each experiment. We describe the results from several experiments below.

Slow-heating Experiments: Figure 1a shows a grain with a pyroxene composition from lunar soil sample 79221. It measures 1.5 µm in size and contains localized Fe nanoparticles (npFe) <50 nm in size. Between room temperature and 575 °C, we did not observe any changes within the grain. At 575 °C, we observed the formation of new npFe in the grain, and an increase in the sizes of those that were present prior to heating. Nanoparticles continued to form and grow larger, up to

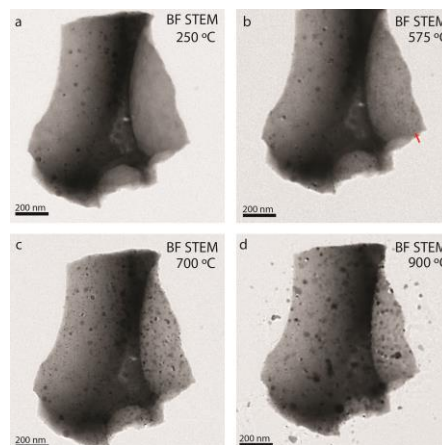


Figure 1: BF STEM images of the grain heated at four different temperatures, a) 250 °C, b) 575 °C, c) 700 °C, and d) 900 °C. The red arrow in panel b) indicates a newly formed npFe particle.

70 nm, during heating to $\sim 1000^\circ\text{C}$ (Fig. 1b,c,d). EDS mapping shows the nanoparticles are composed of Fe.

Single Thermal-Shock Experiments: During rapid heating, we observed the formation of high densities of nanoparticles, both on the grain surfaces and in grain interiors (Fig. 2). The nanoparticles exhibit both spherical and euhedral shapes and EDS mapping revealed that they are composed of Fe (Fig. 2), suggesting they are analogous to npFe particles observed in naturally space weathered lunar and asteroidal soils. The nanoparticles range in size from ~ 5 nm to 47 nm in diameter, with the majority of the npFe measuring < 20 nm in size. We also identified elliptical features that developed in the agglutinitic grains as a result of heating that have low contrast in HAADF imaging, and high contrast in BF imaging. These features are correlated to surface textural changes in the SE images, consistent with vesicles that have formed during the heating event.

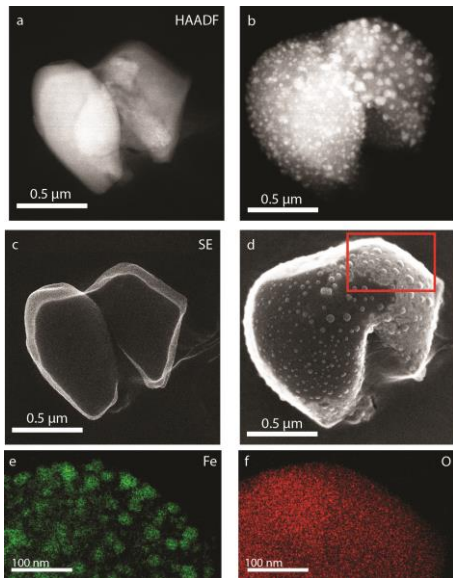


Figure 2: Images of the grain before heating and after heating, respectively, in, a,b) HAADF, c,d) SE. e,f) Fe and O EDS maps from the region outlined in the red box in d).

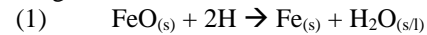
Repeated Thermal-Shock Experiments: After subjecting several grains to multiple thermal shocks, the average size of the npFe particles increases, ranging from 12 nm to 56 nm in diameter. However, the total number of individual nanoparticles decreased between the first and last thermal events.

EELS spectra were collected for npFe protruding from the surface of the host grain, enabling measurement of their oxidation state independent from thickness effects or contributions from Fe in the matrix (Fig. 3). EELS measurements indicate that at least a portion of the nanoparticles are composed of Fe^0 .

Implications for Space Weathering: These experiments produce features in lunar soil that are consistent

with those resulting from space-weathering processes occurring on airless bodies. The npFe formed within these heating experiments is similar in size, shape, distribution, and oxidation state to those identified in lunar soils [2]. The vesicles are similar in shape and size to those identified in samples from Itokawa [9].

There are several hypotheses for the formation of npFe, which include the reduction of Fe^{2+} in the glassy matrix by H implanted by solar wind irradiation, via the following reaction:



Reaction (1) may be favored at high temperatures during micrometeorite impacts. Our experiments were conducted at vacuum, similar to the lunar surface [11] and suggest that the minimum temperature required for npFe formation, if this reaction is viable, is 575°C .

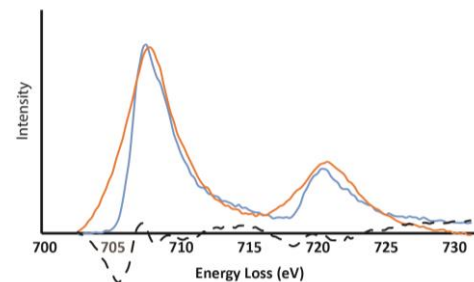


Figure 3: EELS spectra showing the measured nanoparticle in orange, and the simulated fit in blue, from a linear-least squares fitting routine [10]. Residuals shown in black dashed line. This nanoparticle is composed of 100% Fe^0 .

Reaction path (1) is supported by the development of vesiculated textures in the grains, features which are hypothesized to be the product solely of solar-wind implantation [9]. Vesiculated textures are rare in mature lunar soils, however, which have experienced significant irradiation. As such, our work suggests that vesicle formation may require a heating event in the adjacent soil, not only irradiation, to drive the rapid degassing of implanted solar wind H, He, or water (produced by the reaction above) to coalesce into vesicles.

References: [1] Hapke B. (2001) *J. Geophys. Res-Planet.*, 106, 10,039-10. [2] Keller L. P. and McKay D. S. (1997) *Geochim. Cosmochim. Ac.*, 61, 2331-2341. [3] Noble, S. K. et al. 2005, *Meteorit. Planet. Sci.* 40, 397. [4] Noguchi T. et al., 2011, *Science* 333, 1121. [5] Thompson M. S. et al. (2014) *Earth. Planet. Space* 66, 89. [6] Sasaki, S. et al. 2001. *Nature* 410, 555 [7] Loeffler, M. et al. (2009) *J. Geophys. Res – Planet.*, 114:E03003. [8] Noble S. K. et al. (2011) *LPS XXXII*, Abstract #1382 [9] Matsumoto T. et al. (2015) *Icarus* 257, 230-238. [10] Thompson M. S. et al. (2015) *LPS XXXVI*, Abstract #1832. [11] Johnson F. S. (1971) *Rev. of Geophys. Space Phys.*, 9, 813-823.